analytical chemistry

pubs.acs.org/ac Article

Highly Sensitive and Selective Photoelectrochemical Aptasensors for Cancer Biomarkers Based on MoS_2/Au/GaN Photoelectrodes

Danli Hu,[#] Haiyan Cui,[#] Xinyang Wang, Fang Luo, Bin Qiu, Weicheng Cai, Hui Huang, Jian Wang,* and Zhenyu Lin*

Cite This: *Anal. Chem.* 2021, 93, 7341−7347 Read Online

ACCESS | Metrics & More | Article Recommendations

ABSTRACT: An Au/GaN photoelectrode was prepared by sputtering 30 nm thick Au film on the surface of n-type gallium nitride (GaN). When the electrode contacts with multilayered molybdenum disulfide (MoS_2), photogenerated electrons and photogenerated holes transfer to MoS_2 because of the band gap matching of MoS_2 and GaN. The presence of Au promotes charge transfer and results in a greater recombination of electrons and holes; by this means, a more significant suppression of photocurrent can be detected. This characteristic has been coupled with the high selectivity of an aptamer and applied to develop a novel photoelectrochemical aptasensor for cancer biomarkers (alpha-fetoprotein (AFP) as a model). The aptamer of AFP was modified on the surface of the Au/GaN photoelectrode by Au−S bonds, which can bind to the target protein with high selectivity. Then, the transfer process of the charge carriers of GaN to MoS_2 can be blocked by the target protein so that the suppression of photocurrent is reduced. The difference of the photocurrent in the presence and absence of AFP (ΔI) showed a linear relationship with AFP concentration that ranged from 1.0−150 ng/mL (R^2 = 0.9995), and the detection limit was 0.3 ng/mL. The standard addition recovery rates ranged from 85.2 to 91.7%. The method possessed good sensitivity and high selectivity for AFP detection. The developed biosensor can be modified to detect other cancer biomarkers by simply replacing the aptamer used.

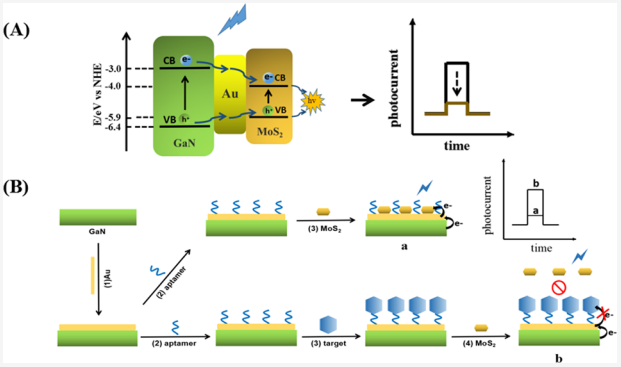

1. INTRODUCTION

Photoelectrochemical (PEC) detection has the advantages of low detection cost, high speed, high sensitivity, simple operation, and so forth. Many sensitive PEC biosensors had been developed for different targets.[1−7] In the design of PEC biosensors, the choice of photoactive materials is particularly important.[5] Gallium nitride (GaN) is a direct band gap semiconductor with a band gap width of 3.39 eV, which is known as the third-generation semiconductor material.[8] Because of its excellent photoelectric activity, chemical stability, nontoxicity, and low cost, GaN has attracted extensive attention.[8−11] However, GaN has rarely been used in the development of PEC sensors because of its excessive chemical stability.[12] Recently, our group explored the potential applications of GaN in the applications of PEC biosensors. An appropriate size of gold nanoparticles (AuNPs) had been modified on the GaN surface, and an AuNPs/GaN Schottky junction can be formed by the energy-level matching of AuNPs and GaN; the photogenerated electrons of GaN can be captured and transferred by the AuNPs to increase the charge migration efficiency, which results in the enhancement of the photocurrent of the system. This character had been coupled with the high selectivity of the aptamer to develop a sensitive aptasensor for CA125 detection.[13] A homogeneous PEC sensor for H_2S detection had been developed based on the band gap matching of iron(III) phthalocyanine-4,4′,4″,4‴-tetrasulfonic acid ($[Fe(III)PcS_4]^+$) and n-type GaN.[12] These examples showed that it is possible to develop high-performance PEC sensors based on GaN by coupling with the materials with a suitable band gap.

Molybdenum disulfide (MoS_2) is a two-dimensional (2D) graphene-like layered structure that has a large active surface area that can facilitate the transportation of electrons and holes.[14−17] The material has the advantages of adjustable optical band gap, high chemical stability, high rare-earth content, nontoxicity, and low cost.[14,18] MoS_2 has been combined with other photoactive materials to enhance the

Received: March 19, 2021
Accepted: April 28, 2021
Published: May 7, 2021

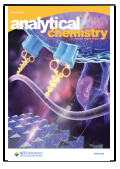

https://doi.org/10.1021/acs.analchem.1c01197
Anal. Chem. 2021, 93, 7341−7347

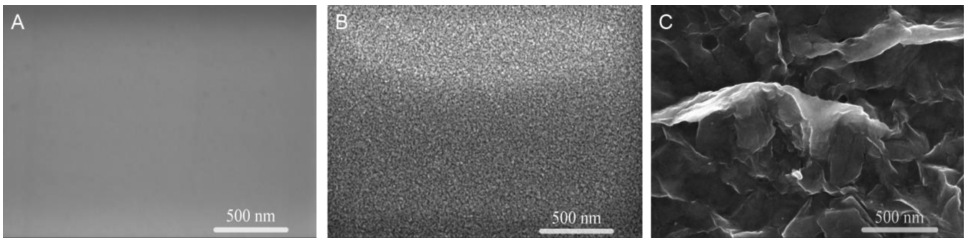

Figure 1. SEM images of (A) GaN, (B) Au/GaN, and (C) multilayered MoS_2 nanosheets.

photoelectric conversion efficiencies of the systems, and it has been widely used in the photocatalytic-related research fields. For example, Chava et al. prepared the hybridization structure of Au-coupled CdS nanorods with few-layered MoS_2 nanosheets, and the MoS_2 nanosheets were used to collect more photogenerated electrons and separate the electrons and holes, which greatly enhanced the hydrogen evolution ability of the system.[19] Pareek et al. designed a p-n junction based on CdS and MoS_2, and the presence of MoS_2 enhanced the stability of CdS and the PEC performance of the system.[20] MoS_2 has been combined with GaN to improve the photocatalytic properties of the materials also. For example, Hassan et al. prepared a MoS_2/GaN heterostructure and used it in PEC water splitting.[18] The electron transfer process between the MoS_2/GaN photoelectrode and the electrolyte interface improved charge separation and transport and enhanced the PEC performance of the system. However, little attention had been paid to develop PEC biosensors based on MoS_2/GaN, although there is good band gap matching between GaN and MoS_2.

In this study, a highly sensitive and selective PEC aptasensor has been developed based on the fact that the photocurrent of the system can be suppressed by the contact between n-type GaN and multilayered MoS_2. Au film was modified on the surface of GaN first, which can capture and transfer the charges from GaN to MoS_2, and it promoted the recombination of electron−hole pairs, so the photocurrent of the system can be suppressed more significantly.[21−26] Furthermore, the presence of Au makes it easy to modify the aptamer on the GaN surface through the Au-S bond.[24] Alpha-fetoprotein (AFP), a glycoprotein produced by the fetal liver and yolk sac and an important clinical tumor marker for hepatocellular carcinoma (HCC), had been chosen as a model target in this study.[27−32] The aptamer of AFP was modified on the surface of the electrode; after the capture of AFP by the aptamer, the process of charge transfer from GaN to MoS_2 can be blocked, which facilitates the reduction of the suppression effect of MoS_2 on the photocurrent of the system. The difference of the photocurrent in the presence and absence of AFP has a certain relationship with the AFP concentration. Based on this, a sensitive PEC biosensor for AFP can be developed. The proposed PEC sensor has been applied for AFP detection in human serum samples with satisfactory results.

2. EXPERIMENTAL SECTION

2.1. Reagents. Multilayered MoS_2 nanosheet dispersion solution with a sheet diameter of 0.02−1.0 μm was purchased from Jiangsu Xianfeng Nanomaterials Technology Co., Ltd. Sodium sulfate (Na_2SO_4) was obtained from Aladdin Reagents Co., Ltd. (Shanghai, China). Epitaxially grown n-type GaN wafers were obtained from Shanghai Dopo Optical Material Co. Ltd. Human serum was obtained from the Affiliated Hospital of Putian University. AFP, carcinoembryonic antigen (CEA), thrombin (TB), bovine serum albumin (BSA), DNA aptamer of AFP, and 0.1 M phosphate buffer saline (PBS, pH = 7.4) were ordered from Shanghai Sangon Biotech Co., Ltd. Also, the AFP aptamer sequence is as follows:[33] 5′-HS-$(CH_2)_6$-GTG-ACG-CTC-CTA-ACG-CTG-ACT-CAG-GTG-CAG-TTC-TCG-ACT-CGG-TCT-TGA-TGT-GGG-TCC-TGT-CCG-TCC-GAA-CCA-ATC-3′.

All chemical reagents were of commercial analytical grade. The experimental water used to prepare the reagent was ultrapure water (18.2 MΩ·cm).

2.2. Apparatus. The detection system for PEC was self-assembled in the laboratory. The photocurrent and electrochemical impedance was obtained using a CHI660D electrochemical workstation (CH Instruments Company of Shanghai, China). PLS-SXE300 Xe lamp (300 W) was ordered from Perfectlight Technology Co., Ltd. (Shanghai, China). The distance between the irradiation source and the photoelectrodes was 6.0 cm. GaN (5.0 mm × 4.0 mm) modified with the Au film was used as the working electrode, the platinum wire electrode was used as the counterelectrode, and the saturated Ag/AgCl electrode was used as the reference electrode. Detection was carried out at room temperature. Scanning electron microscopy (SEM) images were obtained using a Helios G4 CX SEM (Thermo Scientific).

2.3. Fabrication of the PEC Working Electrode. The Au/GaN photoelectrode was obtained by direct-current sputtering 30 nm thick Au film on the n-type GaN epitaxial wafer with a sputtering current of 30 mA using the JCP-350 M3 sputtering instrument (Beijing Technol Co., Ltd.). The GaN epitaxial wafer with the Au-plated film was annealed at 400 °C air for 3 min. Then, the Au/GaN photoelectrode was immersed in 2.0 μM AFP aptamers (200 μL) and incubated at 4 °C for 12 h. The reaction area of the photoelectrode (5.0 mm × 4.0 mm) was 0.2 cm^2, and the rest was stuck with an insulating tape and did not participate in the reaction. After that, the aptamers were attached to the photoelectrode by Au−S bonds. The aptamer/Au/GaN photoelectrode was stored at 4 °C for later use after rinsing with 0.1 M PBS (pH = 7.4).

2.4. Measurement Procedure. Twenty microliters of different concentrations of AFP was dropped into the aptamer/Au/GaN photoelectrode and incubated for 50 min at 37 °C. The electrode was washed with 0.1 M PBS (pH = 7.4), and the difference of the photocurrent of the photoelectrodes in the presence and absence of AFP after the addition of 2.0 μg/mL multilayered MoS_2 nanosheet dispersion solution for 2 min was detected in 0.1 M PBS (pH = 7.4) containing 0.01 M Na_2SO_4. The Xe lamp was used as the excitation light source, and the applied voltage was set to 0.6 V for 10 s on and 10 s off. The procedure for detecting the human serum samples is the same as above.

https://doi.org/10.1021/acs.analchem.1c01197
Anal. Chem. 2021, 93, 7341−7347

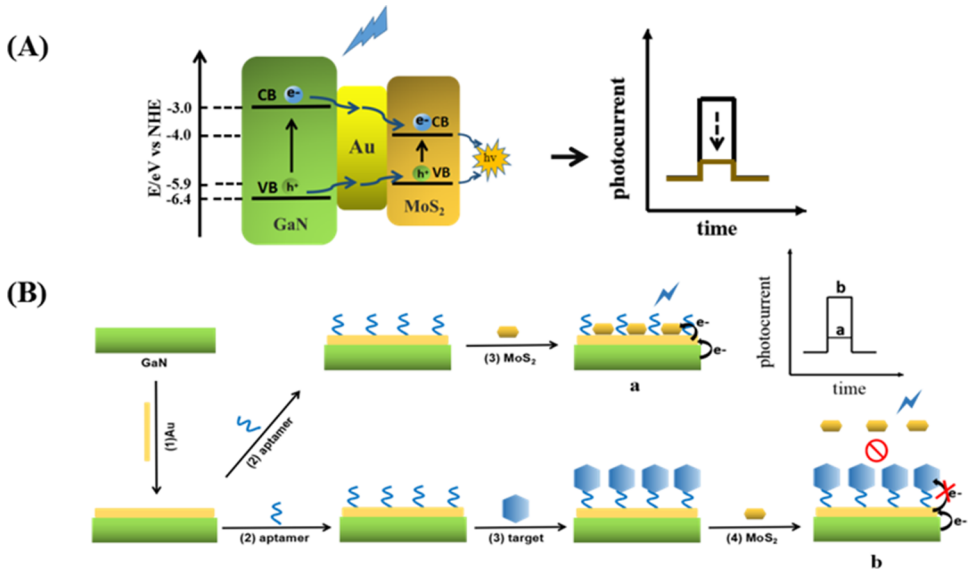

Figure 2. (A) Charge-transfer mechanism in MoS_2/Au/GaN and (B) the AFP detection experiment scheme of the PEC aptasensor.

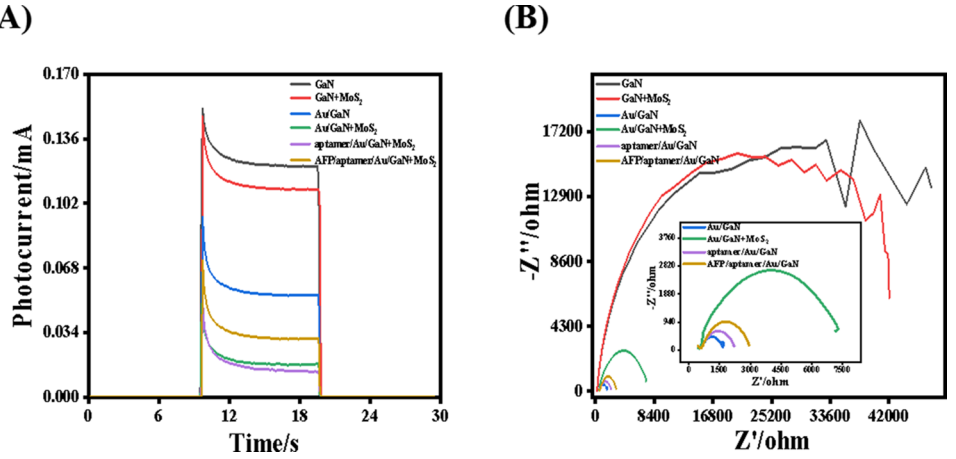

Figure 3. (A) Photocurrent of different modified electrodes obtained in 0.1 M 5 mL of Na_2SO_4 or 0.1 M 5.0 mL of Na_2SO_4 containing 2.0 μg/mL MoS_2 multilayer nanosheets. (B) EIS of different modified electrodes in 5.0 mM $[Fe(CN)_6]^{3/4}$ solution containing 0.1 M KCl or 5.0 mM $[Fe(CN)_6]^{3/4}$ solution containing 0.1 M KCl and 2.0 μg/mL MoS_2 multilayer nanosheets.

The study was approved by the local ethics committee of the Affiliated Hospital of Putian University, and it was in line with the Declaration of Helsinki (2008). All written informed consent was obtained from all participants.

3. RESULTS AND DISCUSSION

3.1. Characterization of the PEC Working Electrode. The morphology of the working electrodes at different stages was characterized by SEM. As shown in Figure 1A, the surface of the commercial GaN epitaxial sheet was smooth and glazed. Figure 1B shows that the surface of GaN modified with the Au film becomes a little rough, and the Au film sputtered on the GaN is uniform. As shown in Figure 1C, the lamellar structure of the multilayered MoS_2 nanosheets is clear and distinct, and the thickness of the nanosheets is about 1−8 nm.

3.2. Principle of the Proposed PEC Biosensor. Figure 2A shows the potential PEC mechanism and charge transfer process. When GaN and MoS_2 are irradiated, the electrons in their valence band (VB) are excited after absorbing the corresponding energy photons, and they transfer to their conduction band (CB), respectively, forming the electron−hole pairs. When two materials are in contact with each other, the band gap positions of n-type GaN (−3.0 to −6.4 eV) and MoS_2 nanosheets (−4.0 to −5.9 eV) match well.[9,12,15] Under the action of the potential gradient, the photogenerated electrons on the CB and the photogenerated holes on the VB of GaN are transferred to the CB and VB of MoS_2, respectively. However, because of the narrower band gap width of MoS_2, the electrons and holes are more likely to recombine, so the photocurrent of the system is suppressed.[12] When there is Au film between GaN and MoS_2, because Au has a good ability of capturing and transferring charge carriers,[25] the transfer of electrons and holes from GaN to MoS_2 will be further promoted, making more electrons and holes recombined and causing greater suppression of the photocurrent of the system. This character can be applied to design a PEC biosensor, and the experimental scheme is shown in Figure 2B. The AFP aptamer was modified on the surface of the Au/GaN photoelectrode through the Au-S bond.[24] When the electrode does not incubate with the target protein (AFP), MoS_2 can contact Au/GaN easily and the electrons and holes of GaN can transfer to MoS_2, and the photocurrent of the

https://doi.org/10.1021/acs.analchem.1c01197
Anal. Chem. 2021, 93, 7341−7347

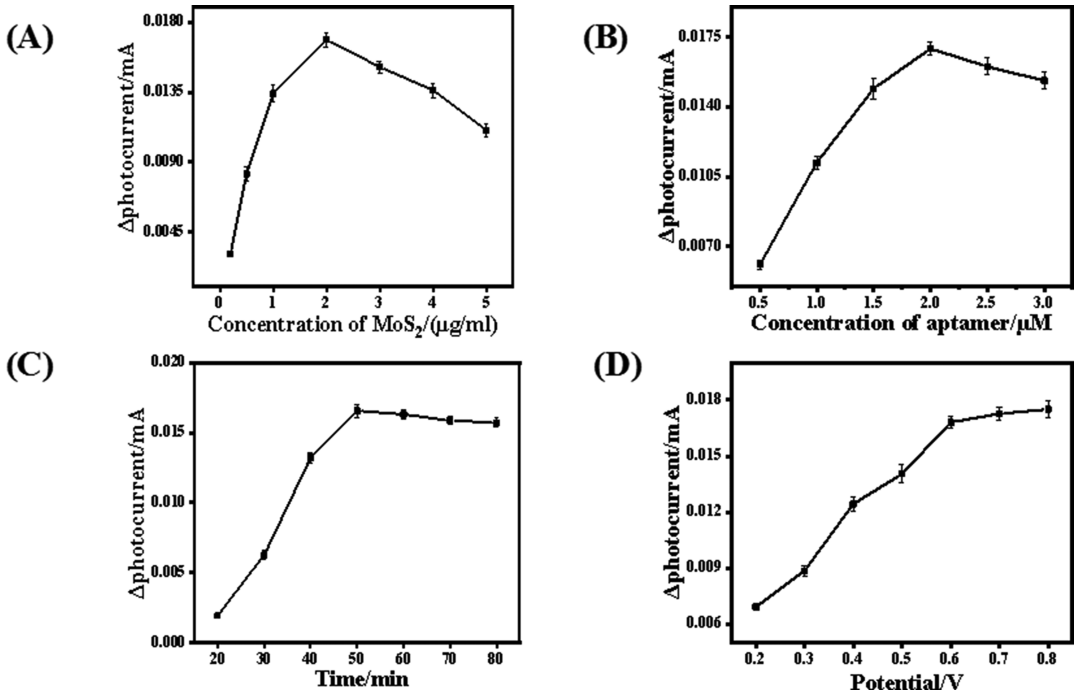

Figure 4. Effects of (A) the concentration of multilayered MoS_2 nanosheets, (B) the concentration of the AFP aptamer, (C) the AFP incubation time, and (D) the applied voltage on the sensor performance (Error bar = RSD (n = 3)). The concentration of the target used in the optimization experiment is 100 ng/mL.

system is suppressed (curve a). After the caption of AFP by the aptamer modified on the electrode surface because the protein has large spatial hindrance, which can block the attachment of MoS_2 on the electrode surface, the photocurrent suppression reduced (curve b). There is a certain relationship between the difference of the photocurrent in the presence and absence of AFP (ΔI) and the concentration of AFP. Based on this, a highly sensitive and selective PEC aptasensor for AFP can be developed.

3.3. Feasibility of the PEC Aptasensor. In order to verify the feasibility of the proposed aptasensor, the photocurrent response of different electrodes was tested (Figure 3A). The highest photocurrent can be detected on GaN, and the photocurrent is suppressed after the GaN contacts MoS_2, indicating that the charge carriers are transferred from GaN to MoS_2. Compared with the photocurrent of GaN, the photocurrent of Au/GaN decreases because Au can shade light. The photocurrent is suppressed more significantly with the addition of MoS_2 in the electrolyte solution using Au/GaN as the photoelectrode. The reason may be because Au promoted the transfer of charge carriers from GaN to MoS_2 and further promoted the recombination of electrons and holes. The photocurrent decreases slightly after the modification of the aptamer, which may be due to the increase of the steric hindrance. However, when the electrode was incubated with the target protein AFP and MoS_2 was then added in the electrolyte solution, the photocurrent value was higher than that without the addition of AFP, indicating that the target protein successfully impeded the contact of MoS_2 to the electrode, that is, the electron and hole recombination caused by charge carriers from GaN to MoS_2 was hindered.

Electrochemical impedance spectroscopy (EIS) was performed to confirm that the sensing surface was successfully fabricated.[6] As shown in Figure 3B, compared with GaN, Au/GaN shows a much smaller electron-transfer impedance (R_{et}) because Au as a conductor has good electric conductivity. This shows the successful modification of the Au film on GaN. After adding MoS_2 in the electrolyte solution, the R_{et} values of the two electrodes increase, indicating that MoS_2 is in contact with the electrodes. The R_{et} value increases slightly after the binding of the aptamer, which may be due to the increase of the steric hindrance. When the electrode incubates the target protein AFP, the R_{et} value increases. This shows that the modification of the protein blocks the electron transfer of the system. These results demonstrated the successful construction of the PEC sensor.

3.4. Optimization of the Experimental Conditions. In order to obtain the best sensing performance, the concentration of multilayered MoS_2 nanosheet dispersion solution, AFP aptamer concentration, the incubation time of the target protein with the modified electrode, and the applied voltage were optimized. Figure 4A describes the influence of the concentration of MoS_2 on ΔI of the system. ΔI increases with the increase of the concentration of MoS_2 first. This is because the photocurrent is suppressed more after the electrode contacts with more MoS_2. Also, ΔI decreases when the MoS_2 concentration exceeds 2.0 μg/mL, which is because too much MoS_2 leads to the increase of impedance and the decrease of photocurrent, and ΔI decreases. Therefore, 2.0 μg/mL is selected as the best condition.

Figure 4B describes the influence of aptamer concentration on ΔI of the system. It can be seen that ΔI increases with the increase of the aptamer concentration because more proteins are attached to the electrode, which prevents more MoS_2 from contacting GaN. When the aptamer concentration is greater than 2.0 μM, ΔI is slightly reduced. This is because more aptamers lead to the increase of the obstruction of electron transfer and the decrease of photocurrent, so the suppressed photocurrent is less and ΔI decreases. Therefore, 2.0 μM had been chosen in the following study.

https://doi.org/10.1021/acs.analchem.1c01197
Anal. Chem. 2021, 93, 7341−7347

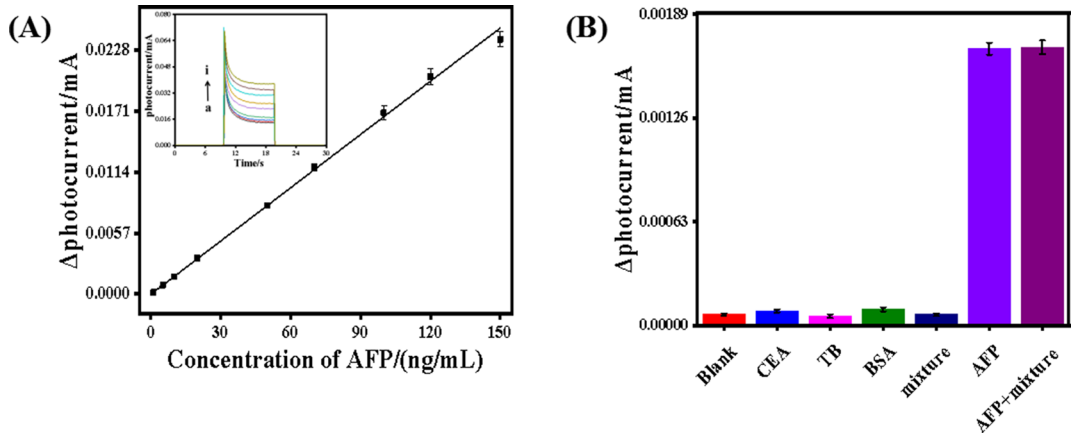

Figure 5. (A) Linear relationship between the difference of the photocurrent in the presence and absence of AFP (ΔI) and AFP concentration in the range of 1.0−150 ng/mL (Error bar = RSD (n = 3)). The inset shows the photocurrent response of different concentrations of AFP, and the concentrations are 1.0 ng/mL (a), 5.0 ng/mL (b), 10 ng/mL (c), 20 ng/mL (d), 50 ng/mL (e), 70 ng/mL (f), 100 ng/mL (g), 120 ng/mL (h), and 150 ng/mL (i), respectively. (B) Specificity of the PEC sensor to detect AFP. The concentrations of CEA, TB, and BSA were obtained as 100 ng/mL. Also, the AFP concentration was 10 ng/mL. Experimental conditions: 2.0 μg/mL multilayered MoS_2 nanosheet dispersion solution, 2.0 μM AFP aptamer, 50 min AFP incubation time, and 0.6 V applied voltage.

Figure 4C describes the optimization of the incubation time of the target protein. It can be seen that the target protein and the aptamer have the best binding degree at 50 min, and ΔI is the highest at this time, so 50 min is selected. As shown in Figure 4D, when the applied voltage is 0.6 V, ΔI increased slowly after protein incubation, indicating that the effect of electron and hole separation became worse at this time, so the applied voltage is selected as 0.6 V.

3.5. Analytical Performance of the Proposed PEC Aptasensor. Under the optimal experimental conditions, the performance of the PEC sensor with different AFP concentrations was investigated. The inset of Figure 5A shows the photocurrent curves of the system after being incubated with different concentrations of target proteins. It can be seen that with the increase of the AFP concentration, the photocurrent of the system increases. As shown in Figure 5A, in the range of 1.0−150 ng/mL, ΔI has a good linear relationship with the AFP concentration. The fitting linear regression equation is as follows:

$$\Delta I\ (\mathrm{mA}) = 1.66 \times 10^{-4}\ C\ (\mathrm{ng/mL}) + 4.34 \times 10^{-6}\ R^2 = 0.9995$$

where C is the AFP concentration and R is the regression coefficient. The detection limit is 0.3 ng/mL (S/N = 3). As shown in Table 1, compared with the previous reported methods, the proposed sensor exhibits a comparable linear range (1.0−150 ng/mL) and detection limit (0.3 ng/mL), indicating that this sensing strategy is a promising method for AFP detection.

In order to study the selectivity of the PEC sensor, possible interfering substances contained in serum such as CEA, TB, BSA, and their mixture were incubated with the modified photoelectrode. The concentration of AFP was 10 ng/mL. Also, the concentrations of CEA, TB, and BSA were obtained as 100 ng/mL. As shown in Figure 5B, the photocurrent response of potential interfering substances and their mixture is almost the same as the blank. Even when mixed interfering substance solution was added together with AFP, none of them obviously interfered with AFP detection. This finding demonstrates that this sensor has good selectivity and anti-interference to the target protein AFP. We also studied the reproducibility of the as-prepared PEC sensor by measuring 100 ng/mL AFP, and the relative standard deviation (RSD) was 4.86% (n = 5). Therefore, the reproducibility of our PEC sensor is satisfactory. Meanwhile, the aptamer/Au/GaN photoelectrode was stored for 1 and 3 weeks under 4 °C, respectively, to detect the stability of the PEC sensor. The results were basically consistent with the freshly prepared photoelectrode, indicating that the sensor has good long-term storage stability.

Table 1. Comparison of Various Methods for AFP Detection

analytical technique	linear range (ng/mL)	detection limit (ng/mL)	references
electrochemical immune sensor	0.01−100	0.099	29
fluorescence aptasensor	10−1000	1.76	34
fluorescence aptasensor	0.5−60	0.16	35
resonance light scattering sensor	5.0−100	0.94	36
electrochemical aptasensor	0.01−100	0.003	37
electrochemical aptasensor	100−100,000	50	38
photoelectrochemical sensor	0.05−20	0.02	39
photoelectrochemical immunosensor	0.05−20	0.0147	40
photoelectrochemical aptasensor	1.0−150	0.3	this work

3.6. Real Sample Analysis. To test the practicability of the PEC aptasensor in the real serum sample, the AFP concentration in six serum samples that were obtained from the Affiliated Hospital of Putian University had been detected. The concentrations of AFP determined in these samples were 6.9, 8.1, 9.7, 82.0, 101.5, and 127.7 ng/mL, respectively, which were very comparable with the reference values (detected by electrochemiluminescence immunoassay) provided by the hospital (Table 2). Also, the standard addition recoveries of AFP in human serum samples were measured to validate the accuracy of the proposed sensor. The results are shown in Table 2, and the recovery rates of AFP in serum ranged from 85.2 to 91.7%, with the relative standard deviation (RSD)

https://doi.org/10.1021/acs.analchem.1c01197
Anal. Chem. 2021, 93, 7341−7347

Table 2. Determination of AFP in Serum Samples with the Fabricated PEC Sensor (n = 3)

sample	detected AFP (ng/mL)	clinical results from hospital (ng/mL)	added (ng/mL)	total found (ng/mL)	RSD (%)	recovery (%)
healthy people	6.9	7.1	20.0	24.4	5.65	87.5
	8.1	8.2	20.0	26.4	4.53	91.7
	9.7	9.8	20.0	26.7	4.92	85.2
patients	82.0	82.3	20.0	99.3	6.27	86.3
	101.5	102.0	20.0	119.2	4.96	88.3
	127.7	128.2	20.0	144.8	5.83	85.6

ranging from 4.53 to 6.27%. The results show that this method has great potential in practical applications.

4. CONCLUSIONS

In summary, a PEC aptasensor based on the MoS_2/Au/GaN photoelectrode has been fabricated for the specific detection of cancer biomarker AFP. When the electrode contacts with multilayered MoS_2, the electrons and holes transfer from GaN to MoS_2. Also, Au has a good ability of capturing and transferring charge carriers, which promotes the transfer of charges from GaN to MoS_2, making more electrons and holes recombined, thus significantly suppressing the photocurrent of the system. The AFP aptamers were attached to the surface of the Au/GaN photoelectrode by Au-S bonds which can bind to the target highly selectively. The presence of AFP blocked the transfer process of the charge carriers; thus, the photocurrent suppression was reduced, which can be employed for AFP detection. The sensor has high sensitivity and high selectivity. The results of quantitative detection for AFP in serum samples are satisfactory. This strategy can be easily modified to detect the other targets if the aptamer had been replaced accordingly.

AUTHOR INFORMATION

Corresponding Authors

Jian Wang − *Ministry of Education Key Laboratory for Analytical Science of Food Safety and Biology, Fujian Provincial Key Laboratory of Analysis and Detection for Food Safety, College of Chemistry, Fuzhou University, Fuzhou, Fujian 350116, China*; Email: jwang@fzu.edu.cn; Fax: 86-0591-22866135

Zhenyu Lin − *Ministry of Education Key Laboratory for Analytical Science of Food Safety and Biology, Fujian Provincial Key Laboratory of Analysis and Detection for Food Safety, College of Chemistry, Fuzhou University, Fuzhou, Fujian 350116, China*; orcid.org/0000-0001-7890-6812; Email: zylin@fzu.edu.cn; Fax: 86-0591-22866135

Authors

Danli Hu − *Ministry of Education Key Laboratory for Analytical Science of Food Safety and Biology, Fujian Provincial Key Laboratory of Analysis and Detection for Food Safety, College of Chemistry, Fuzhou University, Fuzhou, Fujian 350116, China*

Haiyan Cui − *Department of Plastic Surgery, Tongji Hospital of Tongji University, Shanghai 200065, China*

Xinyang Wang − *Ministry of Education Key Laboratory for Analytical Science of Food Safety and Biology, Fujian Provincial Key Laboratory of Analysis and Detection for Food Safety, College of Chemistry, Fuzhou University, Fuzhou, Fujian 350116, China*

Fang Luo − *College of Biological Science and Engineering, Fuzhou University, Fuzhou, Fujian 350116, China*

Bin Qiu − *Ministry of Education Key Laboratory for Analytical Science of Food Safety and Biology, Fujian Provincial Key Laboratory of Analysis and Detection for Food Safety, College of Chemistry, Fuzhou University, Fuzhou, Fujian 350116, China*

Weicheng Cai − *Key Lab of Liaoning IC Technology, School of Biomedical Engineering, Faculty of Electronic Information and Electrical Engineering, Dalian University of Technology, Dalian 116024, China*; orcid.org/0000-0002-8645-944X

Hui Huang − *Key Lab of Liaoning IC Technology, School of Biomedical Engineering, Faculty of Electronic Information and Electrical Engineering, Dalian University of Technology, Dalian 116024, China*; orcid.org/0000-0002-3130-3456

Complete contact information is available at: https://pubs.acs.org/10.1021/acs.analchem.1c01197

Author Contributions

#D.H. and H.C. contributed equally to this work.

Notes

The authors declare no competing financial interest.

ACKNOWLEDGMENTS

This project was financially supported by the National Sciences Foundation of China (21974020, 61774027, 62074023), the cooperative project of production and study in University of Fujian Province (2018Y4007), and the Sciences Foundation of Fujian Province (2018 J01685, 2018 J01682).

REFERENCES

(1) Lin, Y. X.; Zhou, Q.; Tang, D. P.; Niessner, R.; Knopp, D. *Anal. Chem.* **2017**, *89*, 5637−5645.

(2) Fan, G. C.; Han, L.; Zhu, H.; Zhang, J. R.; Zhu, J. J. *Anal. Chem.* **2014**, *86*, 12398−12405.

(3) Wang, L. N.; Ma, W. G.; Gan, S. Y.; Han, D. X.; Zhang, Q. X.; Niu, L. *Anal. Chem.* **2014**, *86*, 10171−10178.

(4) Zhao, W. W.; Xu, J. J.; Chen, H. Y. *Chem. Soc. Rev.* **2015**, *44*, 729−741.

(5) Qiu, Z. L.; Shu, J.; Tang, D. P. *Anal. Chem.* **2018**, *90*, 12214−12220.

(6) Zhang, X.; Chi, K. N.; Li, D. L.; Deng, Y.; Ma, Y. C.; Xu, Q. Q.; Hu, R.; Yang, Y. H. *Biosens. Bioelectron.* **2019**, *129*, 64−71.

(7) Li, H. B.; Qiao, Y. F.; Li, J.; Fang, H. L.; Fan, D. H.; Wang, W. *Biosens. Bioelectron.* **2016**, *77*, 378−384.

(8) Liu, S. J.; Zhao, G.; He, Y. F.; Wei, H. Y.; Li, Y. F.; Qu, P.; Song, Y. M.; An, Y. L.; Wang, X. Y.; Wang, X. X.; Cheng, J. D.; Peng, M. Z.; Zheng, X. H. *ACS Appl. Mater. Interfaces* **2019**, *11*, 35382−35388.

(9) Tangi, M.; Mishra, P.; Tseng, C. C.; Ng, T. K.; Hedhili, M. N.; Anjum, D. H.; Alias, M. S.; We, N.; Li, L. J.; Ooi, B. S. *ACS Appl. Mater. Interfaces* **2017**, *9*, 9110−9117.

(10) Wang, Y. J.; Schwartz, J.; Gim, J.; Hovden, R.; Mi, Z. *ACS Energy Lett.* **2019**, *4*, 1541−1548.

(11) Teker, K. *Sens. Actuators, A* **2014**, *216*, 142−146.

(12) Wang, X. Y.; Zhao, H. N.; Chen, Z. H.; Luo, F.; Guo, L. H.; Qiu, B.; Lin, Z. Y.; Wang, J. *Analyst* **2020**, *145*, 3543−3548.

(13) Hu, D. L.; Liang, H. F.; Wang, X. Y.; Luo, F.; Qiu, B.; Lin, Z. Y.; Wang, J. *Anal. Chem.* **2020**, *92*, 10114−10120.
(14) Li, Y.; DiStefano, J. G.; Murthy, A. A.; Cain, J. D.; Hanson, E. D.; Li, Q.; Castro, F. C.; Chen, X.; Dravid, V. P. *ACS Nano* **2017**, *11*, 10321−10329.
(15) Wu, W. Z.; Wei, C.; Lin, X. C.; Xu, Q. *Chem.–Asian J.* **2018**, *13*, 1293−1296.
(16) Cui, J. B.; Jiang, R.; Lu, W. L.; Xu, S. Y.; Wang, L. Y. *Small* **2017**, *13*, 1602235.
(17) Yin, Z. Y.; Chen, B.; Bosman, M.; Cao, X. H.; Chen, J.; Zheng, B.; Zhang, H. *Small* **2014**, *10*, 3537−3543.
(18) Hassan, M. A.; Kim, M.-W.; Johar, M. A.; Waseem, A.; Kwon, M. K.; Ryu, S. W. *Sci. Rep.* **2019**, *9*, 20141.
(19) Chava, R. K.; Do, J. Y.; Kang, M. *ACS Sustainable Chem. Eng.* **2018**, *6*, 6445−6457.
(20) Pareek, A.; Kim, H. G.; Paik, P.; Borse, P. H. *J. Mater. Chem. A* **2017**, *5*, 1541−1547.
(21) Wang, L. P.; Meng, Y.; Zhang, C. X.; Xiao, H. B.; Li, Y. L.; Tan, Y. M.; Xie, Q. J. *ACS Appl. Mater. Interfaces* **2019**, *11*, 9394−9404.
(22) Tan, Y.; Wang, Y. Y.; Li, M. S.; Ye, X. X.; Wu, T.; Li, C. Y. *Biosens. Bioelectron.* **2017**, *91*, 741−746.
(23) Tan, K. H.; Lee, H. W.; Chen, J.-W.; Dee, C. F.; Majlis, B. Y.; Soh, A. K.; Wu, C.-L.; Chai, S.-P.; Chang, W. S. *J. Phys. Chem. C* **2017**, *121*, 13487−13495.
(24) Vigderman, L.; Zubarev, E. R. *Adv. Drug Deliver Rev* **2013**, *65*, 663−676.
(25) Liu, L. P.; Wang, G. M.; Li, Y.; Li, Y. D.; Zhang, J. Z. *Nano Res.* **2011**, *4*, 249−258.
(26) Wang, P. P.; Dai, W. J.; Ge, L.; Yan, M.; Ge, S. G.; Yu, J. H. *Analyst* **2013**, *138*, 939−945.
(27) Li, G. Y.; Zeng, J. X.; Liu, H. L.; Ding, P.; Liang, J. T.; Nie, X. M.; Zhou, Z. D. *Microchim. Acta* **2019**, *186*, 314.
(28) Yang, X. D.; Zhao, C. L.; Zhang, C. L.; Wen, K.; Zhu, Y. *Sens. Actuators, B* **2020**, *323*, No. 128666.
(29) Xu, T. T.; Chi, B.; Gao, J.; Chu, M. L.; Fan, W. L.; Yi, M. H.; Xu, H.; Mao, C. *Anal. Chim. Acta* **2017**, *977*, 36−43.
(30) Li, Y. K.; Dong, L. Y.; Wang, X. F.; Liu, Y.; Liu, H. L.; Xie, M. G. *Spectrochim. Acta, Part A* **2018**, *196*, 103−109.
(31) Hu, W. H.; Chen, H. M.; Shi, Z. Z.; Yu, L. *Anal. Biochem.* **2014**, *453*, 16−21.
(32) Lu, X. W.; Mei, T.; Guo, Q.; Zhou, W. J.; Li, X. M.; Chen, J. T.; Zhou, X. K.; Sun, N.; Fang, Z. Y. *Microchim. Acta* **2019**, *186*, 2.
(33) Shao, C. G.; Liu, Y. X.; Qi, J. X.; Su, Y.; Chen, Y. H.; Xu, H. G.; Lin, Z. K.; Guan, H. W. *New J. Chem.* **2018**, *42*, 19564−19570.
(34) Bao, B. Q.; Su, P.; Zhu, J.; Chen, J.; Xu, Y.; Gu, B. B.; Liu, Y. F.; Wang, L. H. *Talanta* **2018**, *190*, 204−209.
(35) Xu, S. H.; Feng, X. Y.; Gao, T.; Liu, G. F.; Mao, Y. N.; Lin, J. H.; Yu, X. J.; Luo, X. L. *Anal. Chim. Acta* **2017**, *983*, 173−180.
(36) Chen, F.; Zhang, F.; Liu, Y.; Cai, C. Q. *Talanta* **2018**, *186*, 473−480.
(37) Yang, S. H.; Zhang, F. F.; Wang, Z. H.; Liang, Q. L. *Biosens. Bioelectron.* **2018**, *112*, 186−192.
(38) Li, G. Y.; Li, S. S.; Wang, Z. H.; Xue, Y. W.; Dong, C. Y.; Zeng, J. X.; Huang, Y.; Liang, J. T.; Zhou, Z. D. *Anal. Biochem.* **2018**, *547*, 37−44.
(39) Yang, X. Y.; Li, J. Y.; Fu, J. L. *Anal. Methods* **2015**, *7*, 1328−1332.
(40) Lv, S. Z.; Zhang, K. Y.; Lin, Z. Z.; Tang, D. P. *Biosens. Bioelectron.* **2017**, *96*, 317−323.

https://doi.org/10.1021/acs.analchem.1c01197
Anal. Chem. 2021, 93, 7341−7347